

Predictions of 2019-nCoV Transmission Ending via Comprehensive Methods

Tianyu ZENG, Yunong ZHANG, Zhenyu LI, Xiao LIU, Binbin QIU

School of Data and Computer Science, Sun Yat-sen University, Guangzhou 510006, China

Research Institute of Sun Yat-sen University in Shenzhen, Shenzhen 518057, China

Summary

Since the SARS outbreak in 2003, a lot of predictive epidemiological models have been proposed. At the end of 2019, a novel coronavirus, termed as 2019-nCoV, has broken out and is propagating in China and the world. Here we propose a multi-model ordinary differential equation set neural network (MMODEs-NN) and model-free methods to predict the interprovincial transmissions in mainland China, especially those from Hubei Province. Compared with the previously proposed epidemiological models, the proposed network can simulate the transportations with the ODEs activation method, while the model-free methods based on the sigmoid function, Gaussian function, and Poisson distribution are linear and fast to generate reasonable predictions. According to the numerical experiments and the realities, the special policies for controlling the disease are successful in some provinces, and the transmission of the epidemic, whose outbreak time is close to the beginning of China Spring Festival travel rush, is more likely to decelerate before February 18 and to end before April 2020. The proposed mathematical and artificial intelligence methods can give consistent and reasonable predictions of the 2019-nCoV ending. We anticipate our work to be a starting point for comprehensive prediction researches of the 2019-nCoV.

Article

Coronavirus, a kind of mammalian avian virus, has caused thousands of infected cases. Two of the most famous coronavirus public health events are the severe acute respiratory syndrome (SARS) and the Middle East respiratory syndrome (MERS), which outbreak in 2003 and 2015, respectively. At the end of 2019, another coronavirus¹, termed as 2019-nCoV, was discovered and began transmission in Wuhan City, Hubei Province, China. Because the outbreak position is one of the most important transportation hubs² and the date is close to the annual Spring Festival travel rush² (SFTR), the transmission speed of the virus is faster than that of the SARS in 2003. Additionally, due to the fast development of Chinese transportation facilities construction, the disease can spread interprovincially or even internationally, which makes the people and governments concerned.

Due to its high contagion^{3, 4}, the virus is still spreading fast, and the amounts of patients are still increasing. Thus, the people and governments need to predict the trend of the epidemic and make better decisions to control the transmission. In previous research works, several mathematical models⁵ are proposed, and the ordinary differential equation set (ODEs) driven models have the best interpretability and share the largest ratio. In 1927, Kermack and

McKendrick proposed the susceptible-recovered (SR) model⁶, which can give the dynamic results of the transmission according to the medical information. Later, the extended models, such as the susceptible-exposed-infectious-recovered (SEIR) model⁷, are proposed. However, these models may give inconsistent predictions because of the hypotheses and reality variety. With neural networks⁸⁻¹¹, researchers can generate predictions with the training data⁹, and the artificial intelligence (AI) methodology has deeply changed the modeling methods but avoiding the overfitting problems is another important topic.

In this work, we present three model-free predictive methods and propose an ODE combined predictive neural network, multi-model ODEs neural network (MMODEs-NN), to predict the ending of the transmission. To lay a basis for further discussion, we first get the 2019-nCoV daily transmission data¹² from the Chinese Center for Disease Control and Prevention (CDC) and the CDCs of each province in mainland China from January 10 to February 5, 2020. The data contain the confirmed infected amount, recovered amount and death amount. Then, we also collect the population, density and transportation data of each province during the Chinese SFTR². The three model-free methods, which are based on the sigmoid function^{10, 14}, Gaussian function, and Poisson distribution¹⁵, respectively, only require the daily data. The sigmoid function method requires the total amount of the infected patients, whereas the other two methods require the daily new confirmed data. The MMODEs-NN is a feedforward neural network¹⁶, which takes all the gathered data as the factors and uses the last 4 days data as the test set. The neurons in this neural network are activated by the proposed susceptible-exposed-infected-recovered-susceptible-death (SEIRSD) ODEs, and each of them stores the variable states. Similar to the recurrent neural networks¹⁷, the network can calculate the states for each time step recurrently, and the neuron links can simulate the interprovincial disease transmission in neuron wide propagation and population change according to the transportation data. With certain error evaluation and optimization methods¹⁸, the parameters of the model, such as the disease spreading parameters, can be learned. For more details on the methods and data, please refer to the Method and Supplementary Information sections.

Here we present the prediction results of the 2019-nCoV transmission. Let us denote January 10, 2020, as the 1st day in the training and prediction intervals. When using model-free methods, the results are dependent on the original data. The predictions of these methods are shown in Figs. 1-3, respectively. From these results, one can see that the earliest ending would be the end of February. For the MMODEs-NN, the results are less dependent on the data, so we can train under hypotheses to avoid overfitting and data problems. In general, one has known that the central government of China has taken stronger policies than those in 2003, and we assume that the CDCs in China can count the confirmed patients with no delay. With the help of conjugate gradient method on optimizing the parameters of the disease and transportations, the simulation shows that the ratios between the contact population and the

population-area density in other provinces are 8×10^{-4} , while the ratio in Hubei Province is 0.086 (108x). In this situation, the countrywide total confirmed count would be around 40000. The prediction results are depicted in Fig. 4 and imply that the slowdown would begin on February 7, and the ending would exist before March. However, every disease has a certain time for the researchers to identify. From the latest data, one can see that the data of Hubei Province's total confirmed amount has a boom since January 28, which means the possible existence of this delay. Figs. 5 and 6 suggest the delay situation. The ratio in Hubei Province would be 0.103 (129x), and the countrywide confirmed count would be at the scale of 46000 if the statistical delay is 1 day, while the ratio of Hubei Province would be 0.135 (169x) and the countrywide confirmed count would be at the scale of 58000 if a 2-day delay exists. All the prediction results are listed in Table S7. In these situations, overestimations are acceptable and common in the beginning, and the deceleration date of the transmission would be around February 10, and the ending would happen in March.

What is worth noticing is that the government of Wuhan City declared policies to close the transportation exits of the city¹⁹ on January 23, and later, some other cities in China also announced the similar statements to decelerate the transmission speed. The central government of China also declared other policies to help people and find potential patients under the difficulties, such as prolonging the Spring Festival vacation and conducting strict body temperature measurements in blocks¹⁹. We consider these policies and code them with the proposed network. According to transportation data in the Supplementary Information, the traffic during the 2020 Spring Festival in China decreases by 90% compared with that in 2019. These policies help to control the disease and shrink the total confirmed amounts in each province. We also conduct another simulation without these policies, and the results plotted in Fig. 7 show that the final infected patient amount would reach 450000. In this situation, the most optimistic deceleration date is February 26, and the ending would be around April 28. Thus, these policies work, and their effects are undoubtedly obvious.

In summary, the above numerical prediction results give the expectations on the ending of the transmission. From the experiments, one can see that the model-free methods and the proposed MMODEs-NN can give consistent and confident predictions on the disease and the transmission of the coronavirus would be under control soon. However, every predictive method has its corresponding advantages and shortcomings. The model-free methods show statistical predictions by learning the general form of the developing data, while the proposed MMODEs-NN generates predictions from the simulation by synthesizing the data independency of the ODEs dynamic system and the fitting power of neural networks. For model-free methods, due to the dependency of the data, they are fast to learn the data pattern but would be more likely to make errors if the real-time data are incorrect or have latencies; for the ODEs-NN combined model, it requires more time to train and generate overfitting

problems but it can find the human-like errors in the training data and provide more independent predictions. Both of them have strengths, and the predictions would be more robust and more possible to happen if their results are consistent. Additionally, a variety of uncertain random events happen in real life. For example, the boom in Zhejiang is related to clustering and weak related to the concerned factors in the simulations of MMODEs-NN. However, for the total confirmed amount, our models are relatively accurate, even if the CDC has lowered the standard of judging the confirmed patients since February 9. Thus, we summarize the predicted endings in Table 1 and conservatively estimate that the transmission of the 2019-nCoV would slow down before February 15 and the transmission of this year would finally come to the ending before April. For more detailed data, please refer to the Supplementary Information.

In conclusion, this study has presented comprehensive predictions for the 2019-nCoV transmission ending, providing a guideline for policymaking and a panorama view on the disease future development. Besides the ending, the long treatment cycle, the potential multi-cycle transmission shown in Fig. 1, and the potential high death rate shown in Figs. 4-7 are also worth and important for the medical staff to care about. Based on this work, we expect to do more and deeper predictive researches on the geographical spreading problems with model-free methods and the proposed SEIRSD MMODEs-NN. For it is the first time to apply the comprehensive methods to predict the 2019-nCoV transmission procedure, we anticipate our work to be a starting point for prediction researches of the 2019-nCoV.

Table 1. Final predictions of the 2019-nCoV transmission endings via model-free methods and SEIRSD MMODEs-NN

Method	Sigmoid	Gaussian	Poisson	NN	NN with 1-day delay	NN with 2-day delay	NN without limitation policies
Deceleration	Feb. 4	Feb. 11	Feb. 6	Feb. 7	Feb. 9	Feb. 10	Feb. 26
Ending Date	Feb. 28	Mar. 10	Feb. 29	Feb. 24	Feb. 28	Mar. 3	Apr. 28

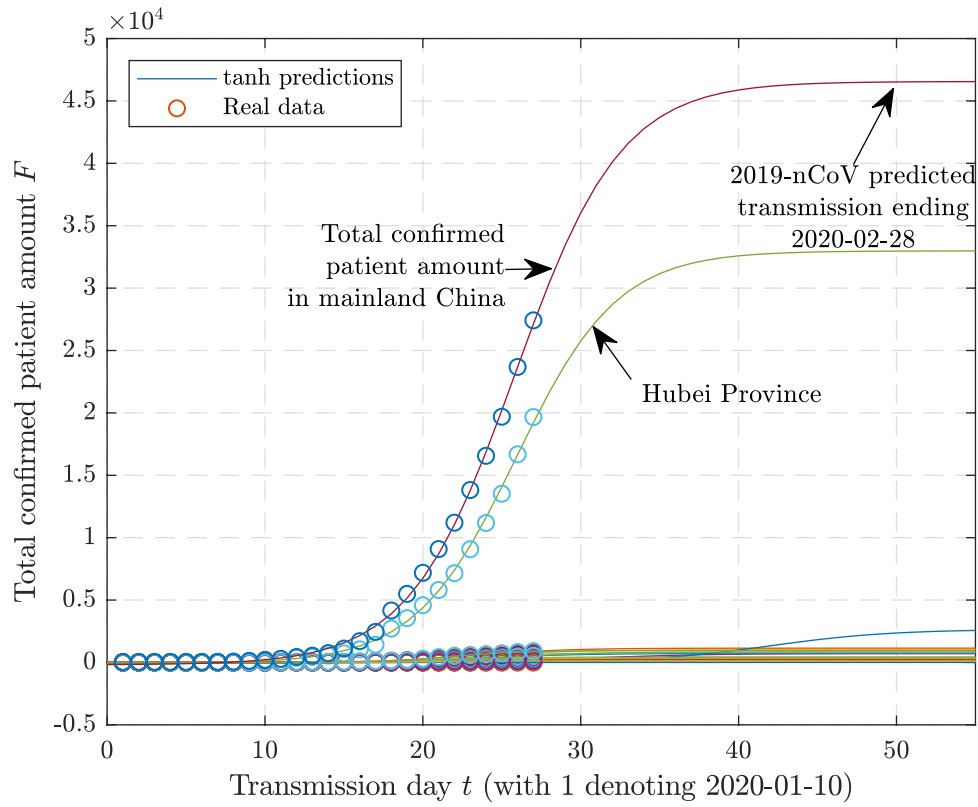


Fig. 1 Predictions of 2019-nCoV transmission ending in mainland China via sigmoid functions. To reduce the count of the function parameters, we adopt the tanh function to fit the data. One can see from the fitting results that the potential transmission ending of the 2019-nCoV would be February 28, 2020, and the final total confirmed amount would be 46000.

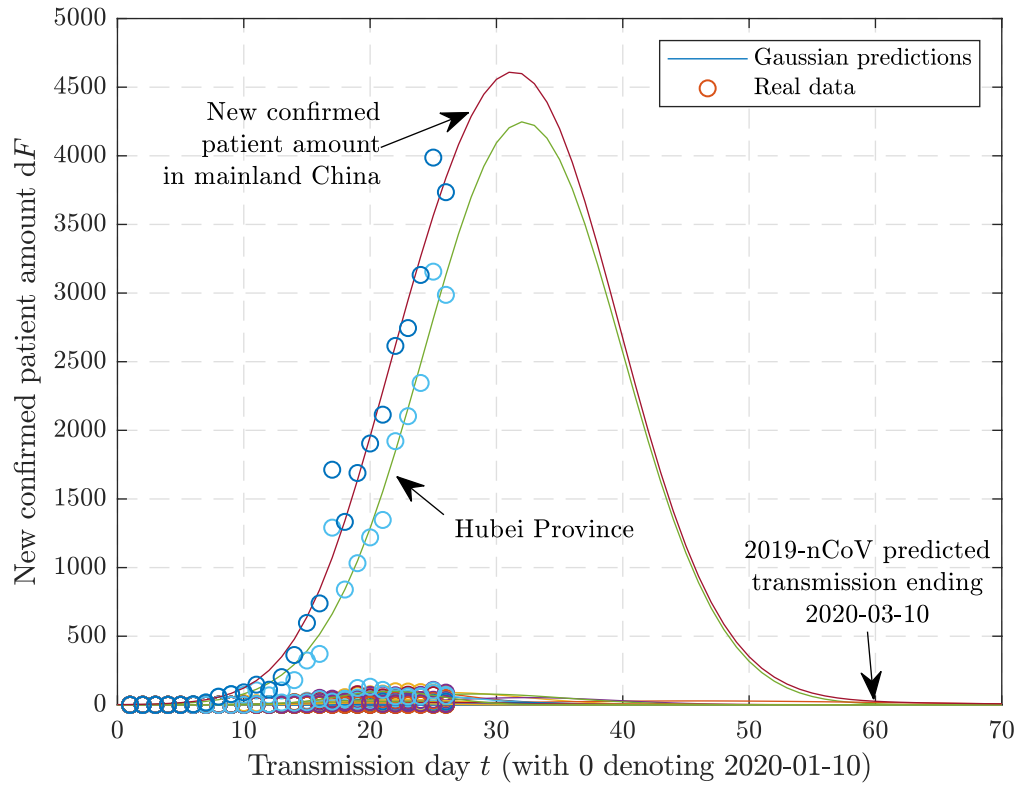


Fig. 2 Predictions of 2019-nCoV transmission ending in mainland China via Gaussian functions. We take the Gaussian function as the target function type. By using new confirmed data, the fitting results can be obtained and indicate that the potential transmission ending of the 2019-nCoV would be March 10, 2020.

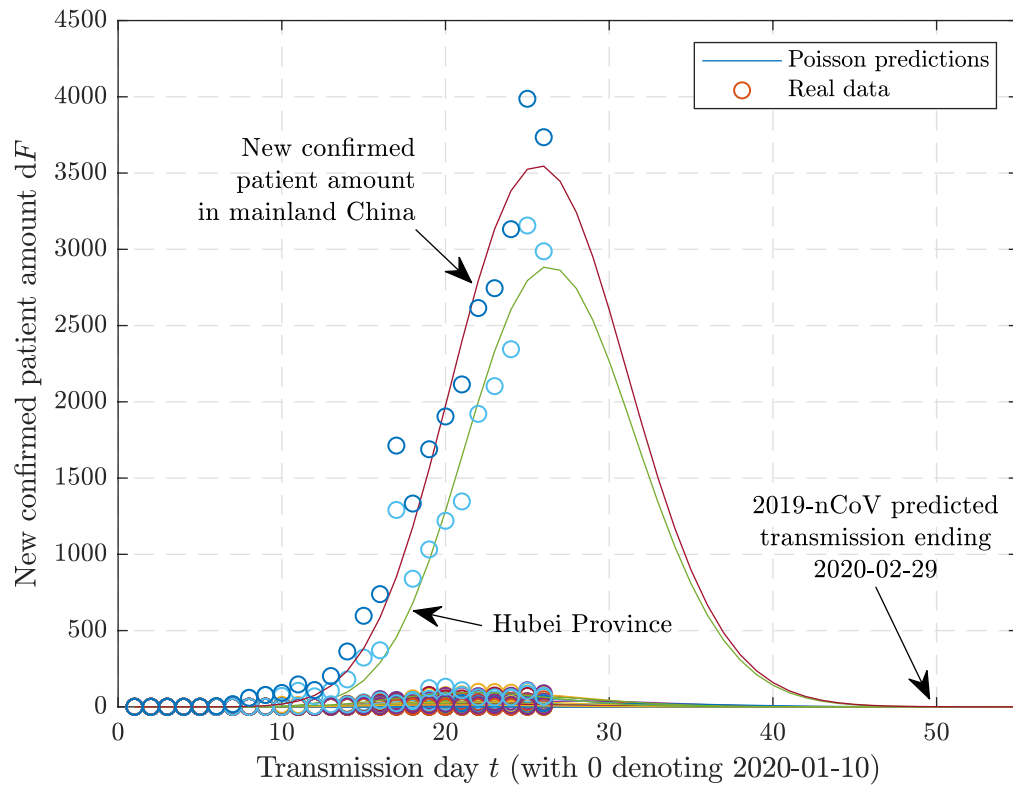


Fig. 3 Predictions of 2019-nCoV transmission ending in mainland China via Poisson distributions. Considering the properties of the Poisson distribution, we construct the continuous Poisson function and fit the provincial data. The fitting results can be obtained and indicate that the potential transmission ending of the 2019-nCoV would be February 29, 2020.

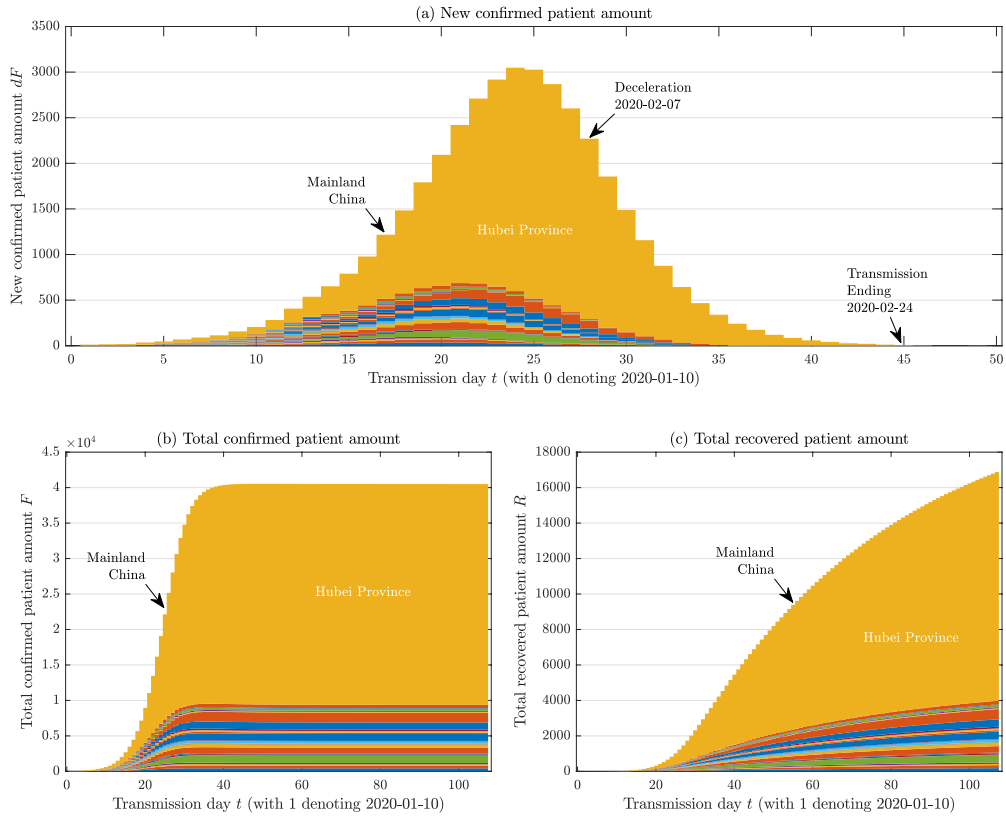


Fig. 4 Predictions of 2019-nCoV transmission ending in mainland China via SEIRSD MMODEs-NN. By using the proposed MMODEs-NN activated by SEIRSD ODEs, we can train the data from January 10 to February 1 and test with the data in the last 4 days. The results in (a) show the potential deceleration would begin on February 7, and the ending would be on February 24, the results in (b) show the potential total confirmed patient amount are at the scale of 40000, and the results in (c) show the recovered patient amount.

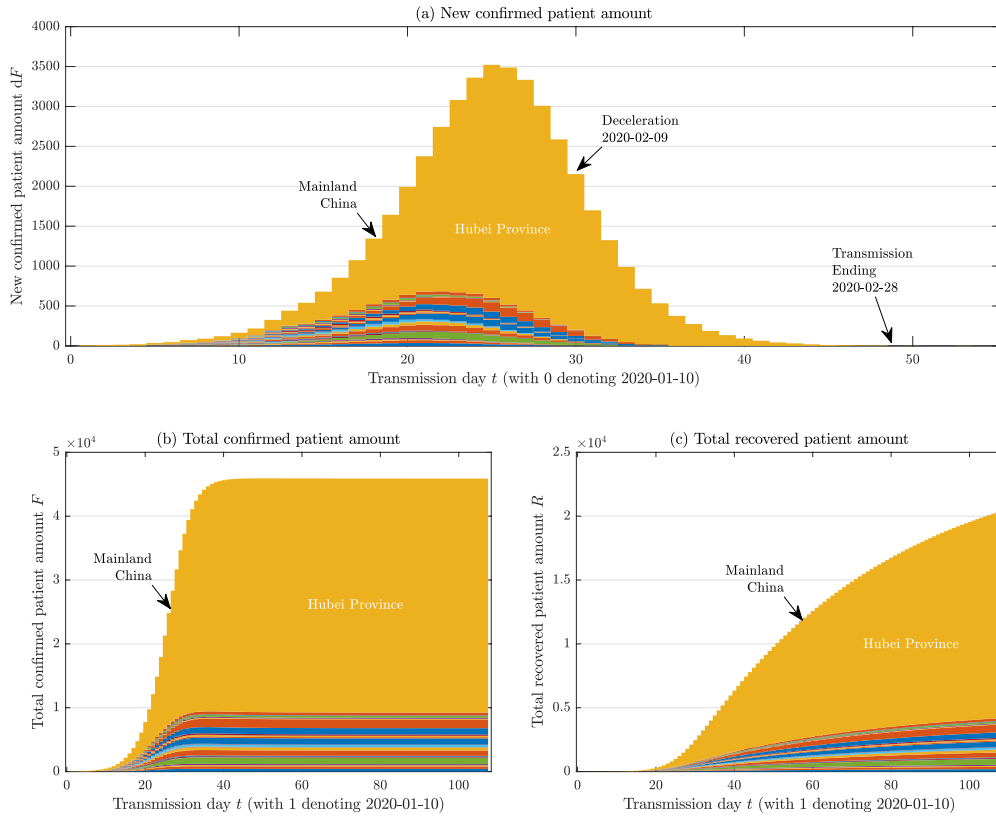


Fig. 5 Predictions of 2019-nCoV transmission ending in mainland China via SEIRSD MMODEs-NN under 1-day statistical delay in Hubei Province. The results in (a) show the deceleration would begin on February 9, and the ending would be on February 28, while (b) shows the potential total confirmed amount would be 46000.

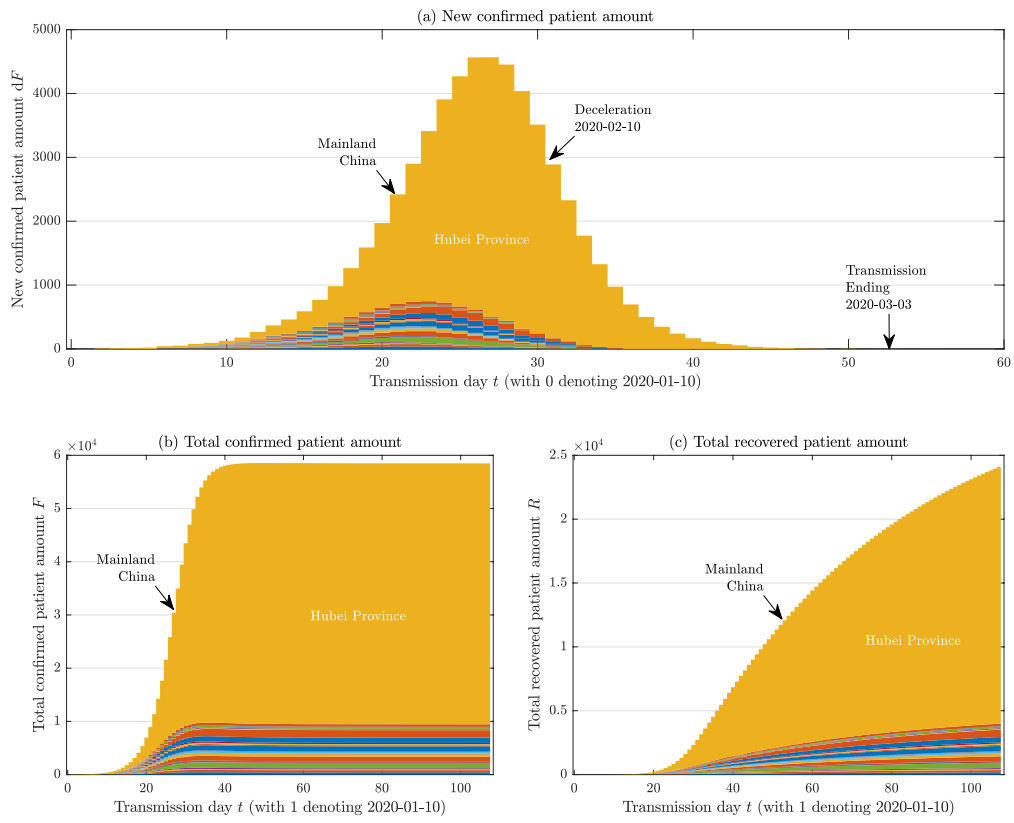


Fig. 6 Predictions of 2019-nCoV transmission ending in mainland China via SEIRSD MMODEs-NN under 2-day statistical delay in Hubei Province. The results in (a) show the deceleration would begin on February 10, and the ending would be on March 3, and figure (b) shows the potential total confirmed amount would be around 58000.

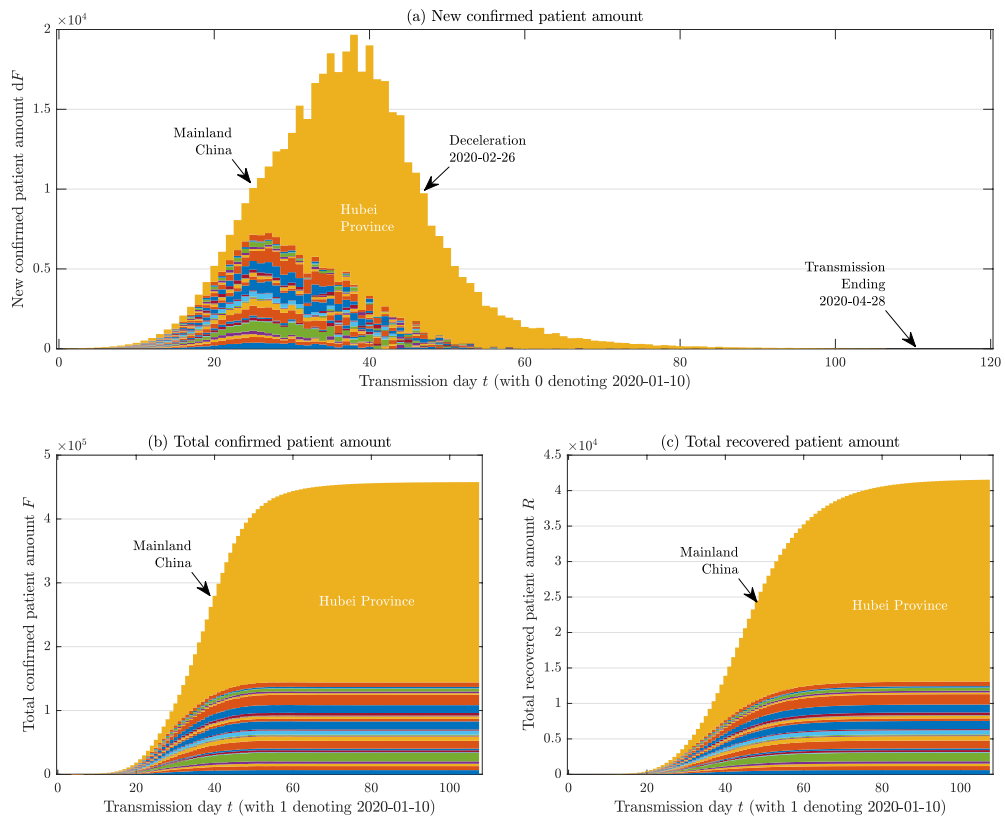


Fig. 7 Predictions of 2019-nCoV transmission ending in mainland China via SEIRSD MMODEs-NN without transportation limitation policies. The results in (a) show the deceleration would begin on February 26, and the ending would be on April 28 in this situation, figure (b) shows the potential total confirmed amount would be around 450000.

Methods

I. Model-Free Methods

In this study, we present three model-free methods to predict the 2019-nCoV transmission ending. They are based on the sigmoid function, Gaussian function, and Poisson distribution, respectively. Here we present their technical details.

A) Sigmoid Function

Sigmoid functions, belonging to a class of S-shaped functions^{10, 14}, include the sigmoid function and tanh function. In the epidemiological models, such as SR and SI models, the results are sigmoid-like functions. In this work, we adopt the tanh function to fit the provincial data. The definition of tanh function is

$$f_1(t, a, b, c, d) = a \tanh(b(t + c)) + d,$$

where t denotes the time, the parameters a , b , c , and d refer to the amplification, scale, initial phase, bias, respectively. By using the confirmed data in Table S1, we can get the fitting results for each province. The countrywide confirmed predictions are shown in Fig. 1, and the detailed data are depicted in Table S2.

B) Gaussian Function

Gaussian distribution is a common existed distribution in real life. From the aspect of time, it means that the probabilities of a certain-theme event will follow a corresponding Gaussian distribution in continuous time. In this work, we assume the probability of an infected patient going to the hospital follows a Gaussian function, which can be written as

$$f_2(t, a, b, c) = a \exp\left(-\left(\frac{x - b}{2c}\right)^2\right),$$

where t denotes the time, a denotes the amplification, b denotes the expectation, and c denotes the standard deviation of the Gaussian distribution. By using the daily newly confirmed data in Table S1, we can get the ending date for each province, and the prediction results are plotted in Fig. 2. The detailed data are depicted in Table S3.

C) Poisson Distribution

Poisson distribution is frequently used as random events distribution¹⁵. In this work, we combine the Poisson distribution with Stirling's approximation²⁰ to get the fitting parameters. The Poisson distribution fitting function is

$$f_3(t, a, b) = \frac{ab^t \exp(t - b)}{t^t \sqrt{2\pi t}},$$

where t denotes the time, a denotes the amplification, and b denotes the expectation in a unit time step. By using the daily newly confirmed data in Table S1, we can get the ending date for each province, and the prediction results are plotted in Fig. 3. The detailed data are depicted in Table S4.

II. SEIRSD ODEs and Multi-Model ODEs Neural Network

The SEIRSD denotes the susceptible-exposed-infected-recovered-susceptible-dead loop. A patient may experience a susceptible period and an exposed period and would be confirmed to be infected. The patient would have a chance to recover and a chance to become dead. The recovered patient might have another chance to get in the loop for another time. For the patient, who is in the exposed state, he/she may become recovered at a certain chance. To describe the loop in a more comprehensive way, here we give the ordinary differential equation set of the SEIRSD, that is,

$$\frac{dS}{dt} = -\beta IS + \theta R, \quad \frac{dE}{dt} = \beta IS - (\alpha + \gamma_1)E, \quad \frac{dI}{dt} = \alpha E - (\gamma_2 + \delta)I, \quad \frac{dR}{dt} = \gamma_1 E + \gamma_2 I - \theta R, \quad \frac{dD}{dt} = \delta I,$$

where the capitalized variables mean the amount of the corresponding words, while the parameters $\alpha, \beta, \gamma_1, \gamma_2, \delta$, and θ denotes the confirmed rate, the transmission rate, the recovery rate of the exposed patients, the recovery rate of the confirmed patients, the death rate, and the recurrence rate, respectively. Like the R_0 value for virus transmission²¹, these parameters are related to the disease properties and can be learned with the MMODEs-NN. In general situations, these parameters would not change rapidly, except for the variation. The hypothesis shared by the ODE-oriented model, which is the total count of the system stays unchanged⁶, can be extended⁷ by the proposed neural network to be the conservation of the involved people ratio. The collected data are the historical provincial total confirmed amounts, the total recovered amounts, and the death amounts, so another two ordinary differential equations can be added, they are,

$$\frac{dF}{dt} = \alpha E, \quad \frac{dC}{dt} = \gamma_2 I,$$

where F and C denote the provincial total confirmed amount and recovered amount of the transmission, respectively.

The ODE neural network¹⁶ is a kind of time-series neural network. The neuron activation methods of this kind are ODE or ODEs instead of nonlinear activation functions. The neuron can store the states of each time step, and their cell states can be activated and propagate to the cells in the next layer. In this work, we present a fully connected feedforward SEIRSD ODEs-activated neural network with multi-model techniques. To make a robust simulation, the proposed network is designed to have 31 SEIRSD-activated neurons in each layer which represents the corresponding time step, and the structure is shown in Fig. S1. The neuron can store some basic information of the corresponding province, such as the population and density. The links between the layers are fully connected to propagate the interprovincial population change during the SFTR. The weights of the links are controlled by the transportation data, which is listed in Table S5. Besides the SEIRSD model in each neuron, the sub-models that we concerned about are the 2020 SFTR model, the noncontact-contact model, and the statistical

delay model. The 2020 SFTR model requires moving-out transportation data. In the last third of January, interprovincial transportations have decreased by 90%, and we formulate it as

$$S_{\text{out}}(t, A, B) = \frac{\mathcal{D}_t(0.9T_{A,B} + 0.2r)S}{100000}, \quad E_{\text{out}}(t, A, B) = \frac{\mathcal{D}_t(0.9T_{A,B} + 0.2r)E}{P_{E_{\text{out}}}}, \quad \mathcal{D}_t = 1 - \frac{P_{\mathcal{D}}}{1 + \exp(-2(t - 12))},$$

where S_{out} and E_{out} denote the amount of the moving-out population and exposed patients, respectively, while T and \mathcal{D} denote the interprovincial transportation ratios and the restriction force, respectively. For the parameters, A and B denote the departure and arrival province, respectively, r denotes a random value, $P_{E_{\text{out}}}$ denotes the exceed rate of the exposed patients, and $P_{\mathcal{D}}$ denotes the shrink rate of the transportation. From the above, one can see that $P_{\mathcal{D}}=0.9$. The noncontact-contact model means that we assume that there is a part of the population who is hard to get in contact with the potential virus carriers, such as the self-isolated people or the students. The amount of these people can be evaluated with a formula, that is,

$$S_c(t, A) = \frac{P_c \mathcal{D}_t \rho(A) S}{\max \rho},$$

where S_c denotes the virus-contact population, ρ denotes the population density and the parameter P_c denotes contact ratio. The S_c will get involved in the SEIRSD ODEs calculation with other variables in the normalized form. As for the statistical delay model, it is used to calculate the delay of patient statistic work. If some confirmed patients do not be found or a period is needed to research the virus, we take the time duration as the statistical delay. In the SEIRSD MMODEs-NN, thanks to the time-flattened structure, we can keep some states of the neurons without dragging the layer wide propagations.

To simplify the calculations, some of the parameters, such as $P_{\mathcal{D}}$, can be directly obtained from the related statistic works. We assume that Hubei Province might have a statistical delay at the beginning of the 2019-nCoV transmission. Thus, in this model, we have 6 virus-related and 1 sub-model parameters to optimize. The error evaluation methods of the historical provincial total confirmed amount and death amount are the mean absolute errors (MAE). With the help of the conjugate gradient optimizer¹⁸, the parameters can be learned, and the data trend can be fitted. Figs. S2 and S3 show the visualizations of the provincial transmissions in mainland China on February 28 and March 31. For more data, please refer to Table S6 for the training details and Table S7 for the predictions.

References

1. Zhou, P., et al. A pneumonia outbreak associated with a new coronavirus of probable bat origin. *Nature*, (2020).
2. Li, J., Ye, Q., Deng, X., Liu, Y., and Liu, Y. Spatial-temporal analysis on Spring Festival travel rush in China based on multisource big data. *Sustainability* **8**, 11, 1184, (2016).
3. Hui, D., et al. The continuing 2019-nCoV epidemic threat of novel coronaviruses to global health—The latest 2019 novel coronavirus outbreak in Wuhan, China. *International Journal of Infectious Diseases* **91**, 264-266, (2020).
4. World Health Organization. Infection prevention and control during health care for probable or confirmed cases of novel coronavirus (nCoV) infection. *Interim Guidance*. Geneva: World Health Organization, (2015).
5. Roberts, F. *Discrete Mathematical Models, with Applications to Social, Biological, and Environmental Problems*, Prentice-Hall Englewood Cliffs, Upper Saddle River, New Jersey, USA, (1976).
6. Kermack, W. and McKendrick, A. A contribution to the mathematical theory of epidemics. *Proceedings of the royal society of London. Series A, Containing papers of a mathematical and physical character* **115**, 772, 700-721, (1927).
7. Li, M. and Muldowney, J. Global stability for the SEIR model in epidemiology. *Mathematical biosciences* **125**, 2, 155-164, (1995).
8. Zhang, Y., Chen, D., and Ye, C. *Toward Deep Neural Networks: WASD Neuronet Models, Algorithms, and Applications*, Chapman and Hall/CRC, Boca Raton, Florida, USA, (2019).
9. Zhang, Y., Guo, D., Luo, Z., Zhai, K., & Tan, H. CP-activated WASD neuronet approach to Asian population prediction with abundant experimental verification. *Neurocomputing* **198**, 48-57, (2016).
10. Zhang, Y., Ding, S., Liu, X., Liu, J., and Mao, M. WASP neuronet activated by bipolar-sigmoid functions and applied to glomerular-filtration-rate estimation. *The 26th Chinese Control and Decision Conference (2014 CCDC)*, 172-177, (2014).
11. Zhang, Y. *Analysis and Design of Recurrent Neural Networks and Their Applications to Control and Robotic Systems*, Ph.D. Thesis, Chinese University of Hong Kong, Hong Kong, (2002).
12. CCDC, *Epidemic Update and Risk Assessment of 2019 Novel Coronavirus*, CCDC, Beijing, China, <http://www.chinacdc.cn/yyrdgz/202001/P020200128523354919292.pdf>, (in Chinese, 2020).
13. Bol, P. and Ge, J. China historical GIS. *Historical Geography* **33**, 150-152, (2005).
14. Hosmer Jr, D., Lemeshow, S., and Sturdivant, R. *Applied Logistic Regression*, John Wiley & Sons, Hoboken, New Jersey, USA, (2013).
15. Consul, P. and Jain, G. A generalization of the Poisson distribution. *Technometrics* **15**, 4, 791-799, (1973).
16. Zhang, Y., Guo, D., and Li, Z. Common nature of learning between back-propagation and Hopfield-type neural networks for generalized matrix inversion with simplified models. *IEEE Transactions on Neural Networks and Learning Systems* **24**, 4, 579-592, (2013).
17. Williams, R., Hinton, G., and Rumelhart, D. Learning representations by back-propagating errors. *Nature* **323**, 6088, 533-536, (1986).
18. Moller, M. *A Scaled Conjugate Gradient Algorithm for Fast Supervised Learning*, Aarhus University, Aarhus, Denmark, (1990).

19. Nature, Coronavirus latest: infections in China pass 20,000. *Nature News*, <https://doi.org/10.1038/d41586-020-00154-w>, (2020).
20. Marsaglia, G. and Marsaglia, J. A New Derivation of Stirling's Approximation to $n!$. *The American Mathematical Monthly* **97**, 9, 826-829, (1990).
21. Liu, T., et al. Transmission dynamics of 2019 novel coronavirus (2019-nCoV). *bioRxiv*, <https://www.biorxiv.org/content/10.1101/2020.01.25.919787v1.abstract>, (2020).

Supplementary Information

More About SEIRSD Model, MMODEs-NN, and Simulations

In the article part, we give a basic view of the SEIRSD model from the ODEs aspect and the corresponding ODEs network. Here we present more detailed illustrations of them.

For the SEIRSD model, Fig. S1(a) displays the structure and the state transition diagram, corresponding to the ODEs of the SEIRSD model that we have shown, which is

$$\frac{dS}{dt} = -\beta IS + \theta R, \quad \frac{dE}{dt} = \beta IS - (\alpha + \gamma_1)E, \quad \frac{dI}{dt} = \alpha E - (\gamma_2 + \delta)I, \quad \frac{dR}{dt} = \gamma_1 E + \gamma_2 I - \theta R, \quad \frac{dD}{dt} = \delta I.$$

For all the variables in the ODEs, we have to change them into the normalized form, and for the parameters, i.e., $\alpha, \beta, \gamma_1, \gamma_2, \delta$, and θ , they are assigned within $[0, 1]$ corresponding to the rate of their meanings. To simulate the transportation population, we add the inputs and outputs to the susceptible and exposed population¹. From the meaning of the state transition diagram, one can see that a person, who is involved with the disease, has a procedure and would be a virus carrier if he/she left the province in the exposed state. With neuron wide propagation, we can see the final interprovincial transmission results.

For the SEIRSD MMODEs-NN, one can see from the structure depicted in Fig. S1(b) that the network is similar to the fully connected neural network. To simulate the true environment in the Chinese Spring Festival travel rush (SFTR), we assume that the interprovincial transportation population during the SFTR is large enough² to ignore the geographical distances, and the weights of each neuron link are obtained with the transportation data displayed in Table S5. What is worth noticing is that each neuron consists of a SEIRSD sub-model, and the interprovincial links can only propagate the transportation population in the form of counts, while the self-links can propagate the neuron states^{3, 4}. For the network initialization, the neurons are loaded with the population and density information of the corresponding province. The network calculates the errors on the training set automatically and adopts the parameters with the best performance on the test set. Similar to the recurrent neural network^{4, 5}, the network shares the parameters and makes predictions by calculating the neuron states in a layer-layer loop. If we want to simulate the delayed situation, we can first propagate and reset the delayed neuron states, which is similar to remove the self-link of the delayed neuron. With the help of numerical optimization methods, such as conjugate gradient⁶ and gradient descent, the parameters in the network can be learned.

After the numerical simulations, whose results are shown in the article, we believe our network can predict the patient counts with 10% errors. These errors might be aroused by the random events that cannot be predicted, such as clustering events happened in Zhejiang and Guangdong. Thus, simply judging the deceleration from the descendent of the newly confirmed patient count would be more likely to make errors. The standard that we judge the starting date of the transmission deceleration is different from the differential methods. We adopt the first day whose new confirmed patient amount is smaller but 1.22 times larger than

the amount on the day before, and larger than 1.22 times the amount on the day after. More specifically, the ratio 1.22 is equal to $11/9$, which is consistent with the error bounds of the proposed network. By judging from the prediction values, we can make sure the true deceleration dates without making error predictions.

We also visualize the prediction results with the map of China. Figs. S2 and S3 depict the predictions of the total confirmed amounts on February 28 and March 31. One can see from the results are close to each other, which means that the transmission of the 2019-nCoV would stop before April. Thus, we conservatively estimate that the transmission of the 2019-nCoV would slow down before February 15 and the transmission of this year would finally come to the ending before April.

However, the ending of the transmission does not mean the vanishment of the 2019-nCoV. The meaning of vanishment means that all the patients are recovered or died, and the infected probabilities are lower than the beginning of the outbreak, while the transmission ending means that the transmission is under control, and the total confirmed amount would not increase in a large scale. In general, after the ending, the virus would be less likely to break out again, but still has the variation probability and arouse multi-cycle transmission, which is important for the medical staff to care about. What is more, from the simulations shown in the article, we can see that the treatment cycle is long, and the potential death rate is high. Although the medical levels in the provinces are not considered, the data from January 10 to February 5 imply the information, and the optimized simulations have shown this warning. For a deeper estimation, we conservatively estimate that the final vanishment would be before August 2020.

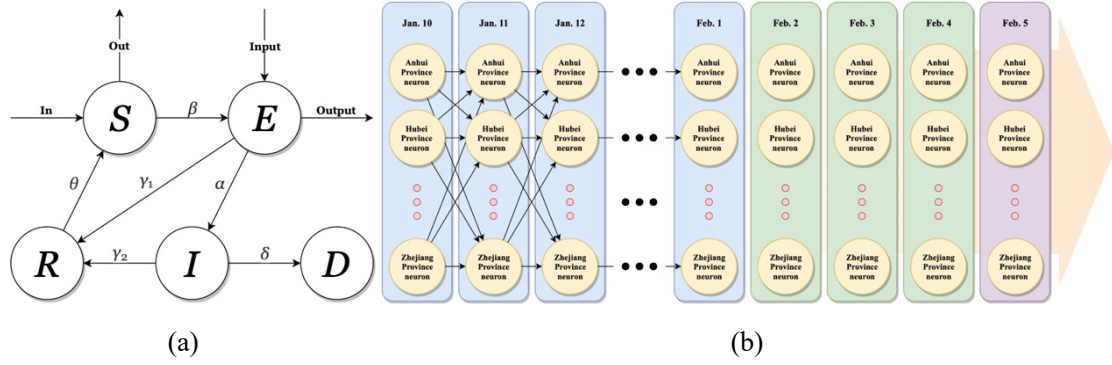


Fig. S1 (a) SEIRSD neuron structure and state transition diagram. (b) Structure of SEIRSD MMODEs-NN for predicting 2019-nCov transmission ending. We first gather the provincial basic information to initialize the network. In each neuron, there is a SEIRSD model. The weights are calculated with the transportation data and the 2020 SFTR model. For each time step, the neurons receive the inputs from the last time step neurons, reinitiate the neurons with the latest states, calculate the SEIRSD model with the noncontact-contact model in the current time step, and propagate to next layer. The test set in the simulations are the latest 4-day data, and the error evaluation method is MAE. The parameters in the network can be learned with conjugate gradient and gradient descent.

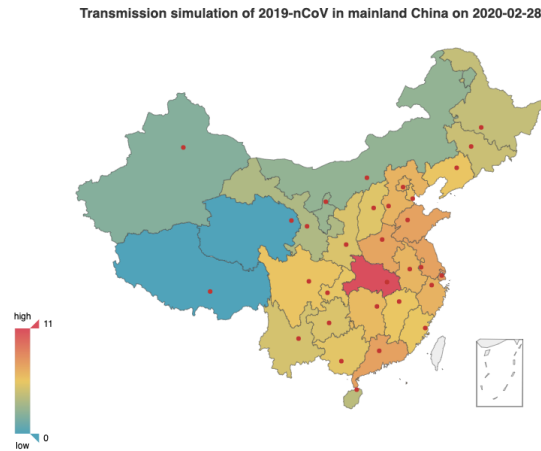


Fig. S2 Total confirmed amounts visualization of 2019-nCoV transmission simulation in mainland China on February 28. This figure is log-scaled. One can see that Hubei Province is of the largest patient amount, while Beijing, Shanghai, Guangdong, Zhejiang, Anhui, and Henan are of a large amount. The provinces, such as Qinghai and Tibet, are of small amounts, which is close to reality.

Transmission simulation of 2019-nCoV in mainland China on 2020-03-31

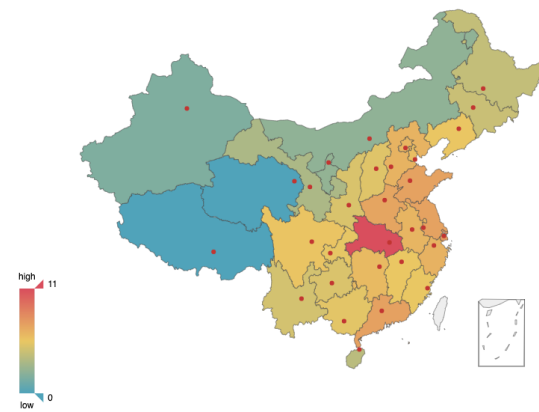


Fig. S3 Total confirmed amounts visualization of 2019-nCoV transmission simulation in mainland China on March 31. This figure is log-scaled. One can see that the results are close to the ones in Fig. S2, which means that the transmission of the 2019-nCoV would stop before April.

Table S1. Historical provincial data of 2019-nCoV confirmed patient amount from January 10 to February 5 (Part 1)

	10	11	12	13	14	15	16	17	18	19	20	21	22	23
AH	0	0	0	0	0	0	0	0	0	0	0	0	1	9
BJ	0	0	0	0	0	0	0	0	0	0	5	10	14	26
CQ	0	0	0	0	0	0	0	0	0	0	0	5	6	9
FJ	0	0	0	0	0	0	0	0	0	0	0	0	1	5
GD	0	0	0	0	0	0	0	0	0	1	14	26	26	32
GS	0	0	0	0	0	0	0	0	0	0	0	0	0	2
GX	0	0	0	0	0	0	0	0	0	0	0	0	2	5
GZ	0	0	0	0	0	0	0	0	0	0	0	0	1	3
HA	0	0	0	0	0	0	0	0	0	0	0	1	5	5
HB	41	41	41	41	41	41	45	62	121	198	270	375	444	549
HE	0	0	0	0	0	0	0	0	0	0	0	0	1	1
HI	0	0	0	0	0	0	0	0	0	0	0	0	4	5
HL	0	0	0	0	0	0	0	0	0	0	0	0	0	2
HN	0	0	0	0	0	0	0	0	0	0	0	1	4	9
JL	0	0	0	0	0	0	0	0	0	0	0	0	0	1
JS	0	0	0	0	0	0	0	0	0	0	0	0	1	5
JX	0	0	0	0	0	0	0	0	0	0	0	2	2	7
LN	0	0	0	0	0	0	0	0	0	0	0	0	2	3
NM	0	0	0	0	0	0	0	0	0	0	0	0	0	0
NX	0	0	0	0	0	0	0	0	0	0	0	0	1	1
QH	0	0	0	0	0	0	0	0	0	0	0	0	0	0
SC	0	0	0	0	0	0	0	0	0	0	0	2	5	8
SD	0	0	0	0	0	0	0	0	0	0	0	1	2	6
SH	0	0	0	0	0	0	0	0	0	0	1	6	9	16
SN	0	0	0	0	0	0	0	0	0	0	0	0	0	3
SX	0	0	0	0	0	0	0	0	0	0	0	0	1	1
TJ	0	0	0	0	0	0	0	0	0	0	0	2	4	5
XJ	0	0	0	0	0	0	0	0	0	0	0	0	0	2
XZ	0	0	0	0	0	0	0	0	0	0	0	0	0	0
YN	0	0	0	0	0	0	0	0	0	0	0	1	1	2
ZJ	0	0	0	0	0	0	0	0	0	0	0	5	10	27
SUM	41	41	41	41	41	41	45	62	121	199	290	437	547	749

The short code for the provinces⁷ can be obtained from Wikipedia (https://en.wikipedia.org/wiki/Provinces_of_China) or China Historical GIS. The data are collected from the CCDC⁸ and CDCs of each province in mainland China.

Table S1. Historical provincial data of 2019-nCoV confirmed patient amount from January 10 to February 5 (Part 2)

	24	25	26	27	28	29	30	31	01	02	03	04	05
AH	15	39	60	70	106	152	200	237	297	340	408	480	530
BJ	36	41	68	80	91	111	121	139	168	191	212	228	253
CQ	27	57	75	110	132	165	206	238	262	275	337	366	389
FJ	10	18	35	59	80	84	101	120	144	159	179	194	205
GD	53	78	111	151	207	277	354	436	535	632	725	813	895
GS	4	4	7	14	19	24	29	35	40	40	55	57	62
GX	23	30	36	46	51	58	78	87	100	111	127	139	150
GZ	3	4	5	7	9	9	12	29	29	38	46	58	64
HA	9	32	83	128	168	206	278	352	422	493	566	675	764
HB	729	1052	1423	2714	3554	4586	5806	7153	9074	11177	13522	16678	19665
HE	2	8	13	18	33	48	65	82	96	104	113	126	135
HI	8	19	22	33	40	43	46	53	62	64	72	80	99
HL	4	9	16	21	33	38	44	59	80	95	121	155	190
HN	24	43	69	100	143	221	277	332	389	463	521	593	661
JL	3	4	5	6	8	9	14	14	17	23	31	42	54
JS	9	18	33	47	70	99	129	168	202	236	271	308	341
JX	18	30	48	72	109	162	162	240	286	333	391	476	548
LN	12	17	22	27	34	39	41	60	64	70	74	81	89
NM	2	7	7	11	15	16	19	20	23	27	34	35	42
NX	2	3	4	7	11	12	17	21	26	28	31	34	40
QH	0	1	3	6	6	7	8	8	9	11	13	15	17
SC	15	28	44	69	90	108	142	177	207	231	254	282	301
SD	15	27	46	75	95	130	158	184	206	230	259	275	307
SH	20	33	40	53	66	96	128	153	169	182	203	219	243
SN	5	15	22	35	46	56	63	87	101	116	128	142	165
SX	6	6	13	20	27	35	39	47	56	56	74	81	81
TJ	8	10	14	23	24	27	31	32	41	48	60	67	69
XJ	2	3	4	5	10	13	14	17	18	21	24	29	32
XZ	0	0	0	0	0	1	1	1	1	1	1	1	1
YN	5	11	16	26	44	55	76	83	93	105	117	122	128
ZJ	43	62	104	128	173	296	428	537	599	661	724	829	895
SUM	1112	1709	2448	4161	5494	7183	9087	11201	13816	16561	19693	23680	27415

The short code for the provinces⁷ can be obtained from Wikipedia (https://en.wikipedia.org/wiki/Provinces_of_China) or China Historical GIS. The data are collected from the CCDC⁸ and CDCs of each province in mainland China.

Table S2. Sigmoid function parameters for predicting 2019-nCoV transmission ending using Table S1

Province	<i>a</i>	<i>b</i>	<i>c</i>	<i>d</i>
AH	362.075	0.170	-24.029	357.012
BJ	171.578	0.127	-22.858	165.851
CQ	225.083	0.167	-21.613	218.971
FJ	115.760	0.183	-21.414	112.812
GD	574.601	0.172	-23.361	570.725
GS	36.712	0.176	-22.280	35.898
GX	95.304	0.142	-22.288	92.118
GZ	46.958	0.194	-24.971	47.061
HA	518.483	0.168	-24.041	509.693
HB	16544.009	0.157	-25.921	16439.011
HE	69.305	0.248	-21.343	68.521
HI	61.566	0.126	-22.555	58.616
HL	356.310	0.136	-30.689	354.362
HN	395.194	0.185	-22.857	388.943
JL	1326.371	0.130	-41.957	1326.191
JS	203.857	0.195	-22.983	201.293
JX	423.549	0.157	-25.130	417.565
LN	50.417	0.162	-21.164	48.906
NM	30.129	0.130	-24.047	29.086
NX	22.541	0.187	-22.392	22.217
QH	11.900	0.133	-23.776	11.437
SC	169.428	0.192	-21.772	166.851
SD	164.396	0.195	-21.291	160.804
SH	132.447	0.188	-21.446	131.138
SN	100.129	0.169	-22.859	97.998
SX	48.673	0.176	-21.987	47.549
TJ	60.534	0.117	-25.262	58.844
XJ	21.384	0.149	-23.517	20.846
XZ	8.579	0.005	-28.764	0.987
YN	66.187	0.237	-20.708	65.263
ZJ	473.293	0.225	-21.729	469.934
SUM	23373.179	0.149	-25.858	23183.127

Table S3. Gaussian function parameters for predicting 2019-nCoV transmission ending using Table S1

Province	<i>a</i>	<i>b</i>	<i>c</i>
AH	60.282	24.464	3.905
BJ	21.802	23.999	5.325
CQ	35.329	21.648	3.967
FJ	19.675	21.073	3.512
GD	95.985	23.162	3.472
GS	6.078	22.315	3.773
GX	13.017	22.655	4.643
GZ	8.966	23.997	2.538
HA	90.518	25.817	4.506
HB	4247.754	32.126	5.548
HE	15.698	20.970	2.635
HI	28.500	45.626	10.441
HL	52.500	32.416	4.996
HN	69.933	23.349	3.777
JL	18.000	30.435	3.538
JS	37.724	23.077	3.398
JX	79.096	28.447	5.084
LN	7.653	21.447	4.219
NM	6.809	34.506	7.779
NX	4.112	24.134	4.348
QH	2.263	31.254	7.018
SC	30.576	21.475	3.265
SD	29.288	21.508	3.662
SH	23.241	21.551	3.535
SN	17.174	24.991	4.762
SX	8.081	21.284	3.353
TJ	6.416	23.915	4.693
XJ	3.445	26.351	5.333
XZ	1.000	19.000	0.174
YN	14.528	20.182	2.636
ZJ	98.858	21.546	2.890
SUM	4230.573	29.214	5.196

Table S4. Poisson distribution parameters for predicting 2019-nCoV transmission ending using Table S1

Province	<i>a</i>	<i>b</i>
AH	741.14	24.14
BJ	273.60	22.30
CQ	432.36	21.38
FJ	232.64	21.17
GD	1163.51	23.42
GS	73.89	22.18
GX	163.69	21.90
GZ	110.48	25.73
HA	1080.13	24.34
HB	37312.83	26.82
HE	166.55	21.68
HI	123.13	24.98
HL	505.63	28.81
HN	854.33	23.17
JL	295.66	32.11
JS	454.93	23.38
JX	855.91	25.32
LN	94.87	21.06
NM	53.28	24.26
NX	50.18	23.03
QH	20.94	23.85
SC	355.68	21.80
SD	351.84	21.44
SH	277.37	21.69
SN	206.98	23.23
SX	94.40	21.52
TJ	81.38	23.22
XJ	39.86	23.42
XZ	1.42	19.30
YN	150.56	20.72
ZJ	1108.19	22.19
SUM	44297.58	25.68

Table S5. Moving-out transportation data of 2020 Chinese Spring Festival travel rush (Part 1)

	AH	BJ	CQ	FJ	GD	GS	GX	GZ	HA	HB	HE	HI	HL	HN	JL
AH	0	2E-02	8E-03	1E-02	2E-02	4E-03	5E-03	7E-03	1E-01	4E-02	2E-02	4E-03	4E-03	2E-02	3E-03
BJ	2E-02	0	8E-03	9E-03	3E-02	8E-03	5E-03	5E-03	7E-02	2E-02	4E-01	1E-02	2E-02	1E-02	1E-02
CQ	1E-02	2E-02	0	1E-02	4E-02	1E-02	1E-02	1E-01	2E-02	7E-02	1E-02	1E-02	3E-03	3E-02	2E-03
FJ	4E-02	2E-02	6E-02	0	1E-01	7E-03	3E-02	9E-02	5E-02	6E-02	1E-02	6E-03	5E-03	6E-02	4E-03
GD	2E-02	1E-02	4E-02	3E-02	0	3E-03	2E-01	6E-02	5E-02	9E-02	7E-03	1E-02	4E-03	2E-01	3E-03
GS	1E-02	3E-02	2E-02	1E-02	2E-02	0	8E-03	1E-02	5E-02	2E-02	2E-02	1E-02	4E-03	1E-02	3E-03
GX	1E-02	1E-02	3E-02	2E-02	4E-01	6E-03	0	9E-02	3E-02	3E-02	2E-02	2E-02	4E-03	1E-01	3E-03
GZ	1E-02	1E-02	2E-01	2E-02	8E-02	3E-03	7E-02	0	2E-02	3E-02	8E-03	1E-02	2E-03	1E-01	2E-03
HA	1E-01	6E-02	1E-02	2E-02	4E-02	1E-02	1E-02	9E-03	0	9E-02	8E-02	1E-02	5E-03	3E-02	4E-03
HB	6E-02	3E-02	7E-02	3E-02	8E-02	1E-02	2E-02	3E-02	1E-01	0	3E-02	9E-03	5E-03	1E-01	4E-03
HE	2E-02	4E-01	5E-03	4E-03	8E-03	4E-03	3E-03	3E-03	7E-02	2E-02	0	4E-03	2E-02	8E-03	1E-02
HI	2E-02	5E-02	4E-02	2E-02	2E-01	1E-02	6E-02	4E-02	5E-02	4E-02	3E-02	0	2E-02	6E-02	1E-02
HL	2E-02	9E-02	7E-03	1E-02	3E-02	7E-03	7E-03	1E-02	3E-02	1E-02	5E-02	2E-02	0	1E-02	2E-01
HN	2E-02	3E-02	4E-02	2E-02	2E-01	8E-03	7E-02	7E-02	4E-02	1E-01	2E-02	1E-02	5E-03	0	4E-03
JL	2E-02	7E-02	6E-03	7E-03	2E-02	6E-03	6E-03	7E-03	3E-02	1E-02	5E-02	1E-02	2E-01	1E-02	0
JS	2E-01	2E-02	1E-02	1E-02	2E-02	1E-02	6E-03	2E-02	9E-02	3E-02	2E-02	3E-03	6E-03	2E-02	4E-03
JX	6E-02	2E-02	2E-02	8E-02	2E-01	1E-02	2E-02	3E-02	5E-02	8E-02	2E-02	9E-03	6E-03	1E-01	5E-03
LN	2E-02	1E-01	7E-03	1E-02	2E-02	6E-03	7E-03	9E-03	4E-02	1E-02	1E-01	1E-02	1E-01	9E-03	2E-01
NM	8E-03	1E-01	4E-03	5E-03	1E-02	3E-02	2E-03	2E-03	2E-02	7E-03	1E-01	8E-03	1E-01	4E-03	7E-02
NX	1E-02	3E-02	1E-02	9E-03	2E-02	2E-01	9E-03	4E-03	4E-02	2E-02	3E-02	7E-03	4E-03	1E-02	3E-03
QH	2E-02	2E-02	2E-02	8E-03	2E-02	4E-01	3E-03	5E-03	7E-02	2E-02	2E-02	9E-03	3E-03	1E-02	1E-03
SC	1E-02	3E-02	3E-01	1E-02	5E-02	3E-02	2E-02	8E-02	3E-02	3E-02	2E-02	1E-02	5E-03	2E-02	4E-03
SD	5E-02	8E-02	9E-03	1E-02	2E-02	8E-03	7E-03	9E-03	1E-01	3E-02	1E-01	6E-03	3E-02	1E-02	2E-02
SH	9E-02	3E-02	2E-02	2E-02	3E-02	7E-03	6E-03	1E-02	5E-02	2E-02	1E-02	6E-03	7E-03	2E-02	5E-03
SN	3E-02	4E-02	3E-02	1E-02	3E-02	1E-01	9E-03	1E-02	1E-01	5E-02	4E-02	1E-02	6E-03	2E-02	5E-03
SX	2E-02	9E-02	1E-02	1E-02	2E-02	8E-03	6E-03	5E-03	1E-01	2E-02	2E-01	1E-02	5E-03	1E-02	5E-03
TJ	3E-02	2E-01	7E-03	7E-03	1E-02	1E-02	7E-03	9E-03	5E-02	1E-02	4E-01	6E-03	2E-02	8E-03	1E-02
XJ	2E-02	4E-02	3E-02	9E-03	3E-02	3E-01	6E-03	5E-03	1E-01	2E-02	3E-02	1E-02	5E-03	1E-02	4E-03
XZ	1E-02	9E-03	6E-02	5E-03	8E-03	5E-02	2E-03	9E-03	4E-02	2E-02	1E-02	2E-03	2E-03	1E-02	6E-04
YN	1E-02	2E-02	8E-02	2E-02	5E-02	6E-03	6E-02	2E-01	3E-02	3E-02	2E-02	7E-03	5E-03	4E-02	4E-03
ZJ	1E-01	1E-02	4E-02	3E-02	2E-02	5E-03	1E-02	1E-01	9E-02	6E-02	9E-03	3E-03	4E-03	6E-02	3E-03

The data in (row A, column B) mean the ratios between the people departing from A to B and the moving-out people in A. The “E” in each item denotes the base of 10, and the “ aEb ” means $a \times 10^b$. For example, 2E-02 denotes 2×10^{-2} . The transportation data are collected from Baidu.

Table S5. Moving-out transportation data of 2020 Chinese Spring Festival travel rush (Part 2)

	JS	JX	LN	NM	NX	QH	SC	SD	SH	SN	SX	TJ	XJ	XZ	YN	ZJ
AH	4E-01	3E-02	5E-03	2E-03	1E-03	7E-04	1E-02	5E-02	8E-02	1E-02	7E-03	6E-03	2E-03	3E-04	6E-03	1E-01
BJ	3E-02	1E-02	3E-02	3E-02	3E-03	1E-03	2E-02	6E-02	2E-02	2E-02	4E-02	7E-02	4E-03	3E-04	7E-03	2E-02
CQ	2E-02	1E-02	5E-03	3E-03	3E-03	3E-03	5E-01	1E-02	1E-02	2E-02	7E-03	5E-03	7E-03	2E-03	4E-02	2E-02
FJ	3E-02	1E-01	6E-03	3E-03	1E-03	6E-04	6E-02	2E-02	3E-02	1E-02	8E-03	5E-03	2E-03	3E-04	3E-02	9E-02
GD	2E-02	9E-02	5E-03	2E-03	7E-04	4E-04	7E-02	1E-02	1E-02	1E-02	4E-03	3E-03	2E-03	1E-04	3E-02	2E-02
GS	4E-02	8E-03	6E-03	3E-02	9E-02	9E-02	9E-02	2E-02	2E-02	3E-01	2E-02	6E-03	5E-02	4E-03	1E-02	2E-02
GX	2E-02	3E-02	7E-03	3E-03	2E-03	1E-03	4E-02	2E-02	9E-03	1E-02	7E-03	4E-03	1E-03	1E-04	7E-02	2E-02
GZ	2E-02	2E-02	3E-03	1E-03	4E-04	4E-04	2E-01	9E-03	9E-03	1E-02	4E-03	2E-03	7E-04	1E-04	2E-01	3E-02
HA	9E-02	2E-02	9E-03	6E-03	4E-03	3E-03	2E-02	1E-01	3E-02	6E-02	6E-02	2E-02	6E-03	3E-04	9E-03	4E-02
HB	5E-02	7E-02	8E-03	6E-03	3E-03	3E-03	4E-02	3E-02	2E-02	3E-02	2E-02	6E-03	6E-03	7E-04	2E-02	4E-02
HE	2E-02	6E-03	3E-02	3E-02	2E-03	8E-04	1E-02	1E-01	6E-03	2E-02	6E-02	1E-01	2E-03	1E-04	4E-03	1E-02
HI	3E-02	3E-02	2E-02	8E-03	3E-03	2E-03	7E-02	3E-02	3E-02	3E-02	2E-02	2E-02	7E-03	2E-04	2E-02	3E-02
HL	3E-02	8E-03	1E-01	1E-01	2E-03	1E-03	2E-02	6E-02	2E-02	1E-02	2E-02	3E-02	3E-03	2E-04	8E-03	2E-02
HN	3E-02	9E-02	6E-03	4E-03	2E-03	2E-03	3E-02	2E-02	2E-02	2E-02	8E-03	4E-03	5E-03	1E-03	2E-02	3E-02
JL	3E-02	7E-03	2E-01	1E-01	3E-03	1E-03	1E-02	5E-02	2E-02	1E-02	2E-02	2E-02	4E-03	3E-04	6E-03	2E-02
JS	0	2E-02	8E-03	3E-03	2E-03	2E-03	2E-02	9E-02	2E-01	2E-02	1E-02	6E-03	3E-03	5E-04	1E-02	1E-01
JX	5E-02	0	7E-03	4E-03	2E-03	2E-03	2E-02	2E-02	4E-02	1E-02	9E-03	5E-03	3E-03	6E-04	1E-02	1E-01
LN	4E-02	7E-03	0	1E-01	2E-03	2E-03	2E-02	7E-02	2E-02	1E-02	2E-02	3E-02	5E-03	4E-04	8E-03	2E-02
NM	1E-02	3E-03	1E-01	0	8E-02	2E-03	9E-03	3E-02	7E-03	1E-01	8E-02	2E-02	2E-03	0E+00	4E-03	7E-03
NX	3E-02	6E-03	6E-03	2E-01	0	1E-02	2E-02	2E-02	2E-02	2E-01	2E-02	5E-03	1E-02	6E-04	1E-02	2E-02
QH	2E-02	4E-03	3E-03	9E-03	2E-02	0	9E-02	2E-02	5E-03	1E-01	1E-02	3E-03	2E-02	4E-02	9E-03	1E-02
SC	2E-02	1E-02	7E-03	5E-03	4E-03	7E-03	0	2E-02	2E-02	6E-02	1E-02	5E-03	1E-02	8E-03	1E-01	2E-02
SD	2E-01	1E-02	4E-02	1E-02	3E-03	2E-03	3E-02	0	3E-02	2E-02	3E-02	4E-02	4E-03	1E-04	9E-03	3E-02
SH	4E-01	3E-02	9E-03	3E-03	1E-03	6E-04	2E-02	3E-02	0	1E-02	8E-03	6E-03	3E-03	2E-04	1E-02	2E-01
SN	4E-02	1E-02	9E-03	6E-02	4E-02	1E-02	1E-01	4E-02	2E-02	0	1E-01	8E-03	2E-02	3E-03	1E-02	2E-02
SX	3E-02	8E-03	1E-02	8E-02	6E-03	3E-03	3E-02	6E-02	1E-02	1E-01	0	3E-02	2E-03	2E-04	9E-03	2E-02
TJ	2E-02	6E-03	3E-02	2E-02	3E-03	2E-03	1E-02	8E-02	1E-02	1E-02	4E-02	0	5E-03	4E-04	7E-03	1E-02
XJ	3E-02	5E-03	8E-03	2E-02	2E-02	3E-02	1E-01	3E-02	1E-02	8E-02	1E-02	6E-03	0	1E-03	9E-03	2E-02
XZ	9E-03	5E-03	3E-03	9E-04	3E-03	1E-01	4E-01	1E-02	4E-03	6E-02	6E-03	2E-03	6E-03	0	5E-02	6E-03
YN	2E-02	2E-02	7E-03	4E-03	2E-03	1E-03	3E-01	2E-02	1E-02	2E-02	8E-03	5E-03	3E-03	2E-03	0	3E-02
ZJ	1E-01	1E-01	5E-03	2E-03	8E-04	3E-04	4E-02	2E-02	9E-02	1E-02	5E-03	2E-03	1E-03	0E+00	3E-02	0

The data in (row A, column B) mean the ratios between the people departing from A to B and the moving-out people in A. The “E” in each item denotes the base of 10, and the “ aEb ” means $a \times 10^b$. For example, 2E-02 denotes 2×10^{-2} . The transportation data are collected from Baidu.

Table S6. Training results of SEIRSD MMODEs-NN

	α	β	γ_1	γ_2	δ	θ	P_C	Hubei P_C	Total confirmed MAE
No delay	1.00	0.58	0.39	0.01	0.009	0.00	0.0008	0.0864	1611.74
One-day	1.00	0.59	0.41	0.01	0.009	0.00	0.0008	0.1032	1296.33
Two-day	1.00	0.60	0.38	0.01	0.009	0.00	0.0008	0.1352	1331.33
No transportation limitation policies	1.00	0.80	0.30	0.01	0.100	0.00	0.0008	0.0864	9867.48

Table S7. Total Confirmed amount prediction results of SEIRSD MMODEs-NN Simulations in mainland China

Date	No delay	One-day delay	Two-day delay	No transportation limitation policies	Reality
2020/2/1	16175	14866	14247	36915	13816
2020/2/2	19093	17947	17658	44973	16561
2020/2/3	22141	21308	21566	54092	19693
2020/2/4	25168	24830	25836	64161	23680
2020/2/5	28036	28318	30402	74857	27415
2020/2/6	30638	31652	34970	86275	31211
2020/2/7	32908	34661	39423	98637	34598
2020/2/8	34763	37249	43461	111145	37198
2020/2/9	36251	39402	46974	124667	40171
2020/2/10	37408	41101	49863	139896	42638
2020/2/11	38284	42426	52191	154289	44653
2020/2/12	38928	43416	53964	170937	--
2020/2/13	39395	44132	55290	188166	--
2020/2/14	39735	44666	56265	206676	--
2020/2/15	39976	45042	56961	224008	--
2020/2/16	40150	45316	57461	242632	--
2020/2/17	40270	45504	57808	262303	--
2020/2/18	40356	45639	58048	279664	--
2020/2/19	40415	45732	58215	298669	--
2020/2/20	40457	45797	58328	315552	--
2020/2/21	40484	45841	58405	332321	--
2020/2/22	40505	45873	58462	347140	--
2020/2/23	40517	45893	58495	361771	--
2020/2/24	40525	45905	58517	373450	--
2020/2/25	40530	45914	58533	384479	--
2020/2/26	40530	45920	58540	394220	--
2020/2/27	40530	45926	58545	401930	--
2020/2/28	40532	45926	58546	408992	--
2020/2/29	40533	45926	58547	415307	--
2020/3/1	40533	45926	58547	420487	--
2020/3/2	40533	45926	58547	424979	--
2020/3/3	40533	45926	58547	429093	--
2020/3/4	40533	45926	58547	432650	--
2020/3/5	40533	45926	58547	435338	--
2020/3/6	40533	45926	58547	437927	--
2020/3/7	40533	45926	58547	440011	--
2020/3/8	40533	45926	58547	441960	--
2020/3/9	40533	45926	58547	443753	--

The CDC of China has lowered the standard to judge the confirmed infected patients since February 9, 2020. However, the error rates between the reality and the predictions are less than 10%, and the values of the reality are likely to approach the two-day delayed predictions.

References

1. Li, M. and Muldowney, J. Global stability for the SEIR model in epidemiology. *Mathematical biosciences* **125**, 2, 155-164, (1995).
2. Li, J., Ye, Q., Deng, X., Liu, Y., and Liu, Y. Spatial-temporal analysis on Spring Festival travel rush in China based on multisource big data. *Sustainability* **8**, 11, 1184, (2016).
3. Zhang, Y. *Analysis and Design of Recurrent Neural Networks and Their Applications to Control and Robotic Systems*, Ph.D. Thesis, Chinese University of Hong Kong, Hong Kong, (2002).
4. Williams, R., Hinton, G., and Rumelhart, D. Learning representations by back-propagating errors. *Nature* **323**, 6088, 533-536, (1986).
5. Zhang, Y., Guo, D., and Li, Z. Common nature of learning between back-propagation and Hopfield-type neural networks for generalized matrix inversion with simplified models. *IEEE Transactions on Neural Networks and Learning Systems* **24**, 4, 579-592, (2013).
6. Moller, M. *A Scaled Conjugate Gradient Algorithm for Fast Supervised Learning*, Aarhus University, Aarhus, Denmark, (1990).
7. Bol, P. and Ge, J. China historical GIS. *Historical Geography* **33**, 150-152, (2005).
8. CCDC, *Epidemic Update and Risk Assessment of 2019 Novel Coronavirus*, CCDC, Beijing, China, <http://www.chinacdc.cn/yyrdgz/202001/P020200128523354919292.pdf>, (in Chinese, 2020).